Commun Nonlinear Sci Numer Simulat 48 (2017) 439–453

Contents lists available at ScienceDirect

Commun Nonlinear Sci Numer Simulat

journal homepage: www.elsevier.com/locate/cnsns

Research paper

# A HAM-based wavelet approach for nonlinear ordinary differential equations

Zhaochen Yang[c], Shijun Liao[a,b,c,*]

[a] State Key Laboratory of Ocean Engineering, Shanghai 200240, China
[b] Collaborative Innovation Centre for Advanced Ship and Deep-Sea Exploration (CISSE), Shanghai 200240, China
[c] School of Naval Architecture, Ocean and Civil Engineering, Shanghai Jiao Tong University, Shanghai 200240, China

ARTICLE INFO

*Article history:*
Received 5 April 2016
Revised 31 October 2016
Accepted 2 January 2017
Available online 4 January 2017

*Keywords:*
Wavelet
Homotopy analysis method
HAM
Generalized Coiflet-type wavelet
Bratu equation

ABSTRACT

Based on the homotopy analysis method (HAM) and the generalized Coiflet-type orthogonal wavelet, a new analytic approximation approach for solving nonlinear boundary value problems (governed by nonlinear ordinary differential equations), namely the wavelet homotopy analysis method (wHAM), is proposed. The basic ideas of the wHAM are described using the one-dimensional Bratu's equation as an example. This method not only keeps the main advantages of the normal HAM, but also possesses some new properties and advantages. First of all, the wHAM possesses high computational efficiency. Besides, based on multi-resolution analysis, it provides us a convenient way to balance the accuracy and efficiency by simply adjusting the resolution level. Furthermore, different from the normal HAM, the wHAM provides us much larger freedom to choose the auxiliary linear operator. In addition, just like the normal HAM, iteration can greatly accelerate the computational efficiency of the wHAM without loss of accuracy.



## 1. Introduction

Since the homotopy analysis method (HAM) was proposed in 1992 by Liao [1–7], this powerful and easy-to-use analytical tool has been widely and successfully used to solve many nonlinear problems in science and industry [8–18]. Compared with perturbation techniques [19,20] and some non-perturbative techniques (such as the artificial small parameter method [21], the $\delta$-expansion method [22], the Adomian's decomposition method [23] and so on), the HAM has the following advantages [3]:

(1) Based on the homotopy, a basic concept in topology, the HAM is independent of any small/large physical parameters at all;
(2) Unlike other analytic techniques, the HAM provides us a convenient way to guarantee the convergence of solution series;
(3) It can provide us extremely large freedom to choose equation type of linear sub-problems and the corresponding base functions of solution.

All of these advantages have been illustrated by various examples [2,3]. Thanks to all of the above advantages, it becomes possible to gain convergent series solution of many strongly nonlinear differential equations through the HAM by

* Corresponding author.
*E-mail address:* sjliao@sjtu.edu.cn (S. Liao).

http://dx.doi.org/10.1016/j.cnsns.2017.01.005
1007-5704/

choosing proper base functions and the corresponding auxiliary linear operator, and especially a proper value of the so-called convergence-control parameter.

However, due to the nonlinearity, as the order of approximation increases, the computational complexity of the high-order equations grows rapidly. Therefore, just as noted in [3,24], the CPU time to gain the high-order approximation often increases exponentially for the normal HAM. To improve the computational efficiency, some techniques have been developed, such as the truncation technique (called tHAM) [3,24], the iteration approach (called iHAM) [3,24], the spectral homotopy analysis method (called sHAM) [25–29] and so on. It is found that, in most cases, the truncation and iteration technique can greatly accelerate the convergence of the solution. However, it should be emphasized that the iteration technique must be based on the truncation of the right-hand side term of the high-order equation [24]. Besides, in the frame of the normal HAM, the solution expression is strongly dependent upon the auxiliary linear operator. For example, if the linear operator is chosen in the form of $\mathscr{L}[\phi] = \frac{\partial^2\phi}{\partial x^2} + \phi$, the trigonometric function should be selected as the base function for the solution expression. If not, say, the linear operator is chosen in the form of $\mathscr{L}[\phi] = \frac{\partial^2\phi}{\partial x^2} + \phi$ while polynomial or exponential function is used as the base function, it is impossible to gain the solution correctly. The sHAM [25–29] overcomes some of the problems by using Chebyshev polynomials as base functions and solving high-order deformation equations by the spectral method.

Therefore, without doubt, the base function plays a significant role for efficiently obtaining a good approximation of a highly nonlinear equation. Our purpose is to develop such a new HAM approach that:

(A) It is insensitive to the choice of the auxiliary linear operator so that it can be more flexible and adaptive to choose the auxiliary linear operator;
(B) The exponential expansion of the right-hand side term in high-order deformation equation can be overcome in a convenient way;
(C) It can provide a convenient way to balance the computational efficiency and approximative accuracy so that an acceptable approximation can be obtained efficiently.

For these purposes, the generalized Coiflet-type orthogonal wavelet developed by Wang and Zhou et al. [30–34] is applied as base functions to develop such a new HAM approach. The history of wavelet theory and its applications can be traced back to Morlet [35], a French geophysicist who first put forward the concept of wavelet transformation in 1974, and Haar [36], who first constructed a wavelet orthonormal basis (called Haar's orthogonal wavelet) in 1910. Since then, the wavelet theory has been widely applied to pure mathematics, signal analysis, image processing, seismic prospecting, medical science, chemistry, biology, solid mechanics, turbulent and electromagnetism, etc [30]. The early applications of wavelet in differential equations could be traced back to 1990s [37–39]. However, as the theory of wavelet method for differential equations was not established, many basic problems such as boundary leaping and computation of connection coefficients were needed to solve [30,40,41]. Wang and Zhou et al. [30–34] developed the generalized Coiflet-type orthogonal wavelet and proposed a new boundary extension technique [30,34,41–43] similar to Taylor's expansion, and Chen et al.[44] put forward a high accuracy algorithm in accordance with the basic operational rules of wavelet analysis. Now, the wavelet method becomes a widely applied numerical technique with high accuracy for differential equations.

In this paper, we propose a HAM-based approach, namely the wavelet homotopy analysis method (wHAM), which successfully combines the homotopy analysis method and the generalized Coiflet-type orthogonal wavelet. In Section 2, some related theories of the generalized Coiflet-type orthogonal wavelet are introduced. In Section 3, the basic ideas of wHAM is described by using the Bratu's problem as an example. In Section 4, numerical results are given to illustrate the validity and computational efficiency of the wHAM. In Section 5, the concluding remarks about the wHAM are described.

## 2. Wavelet approximation

For the generalized Coiflet-type orthogonal wavelet, the scaling function $\varphi(x)$ and wavelet function $\psi(x)$ possess the following properties [30,34]:

$$(a)\ \varphi(x) = \sum_{l\in\mathbb{Z}} p_k \varphi(2x-l); \tag{1}$$

$$(b)\ \psi(x) = \sum_{l\in\mathbb{Z}} (-1)^k p_{1-k} \psi(2x-l); \tag{2}$$

$$(c)\ M_n = M_1^n, \quad for\ 0 \le n < N; \tag{3}$$

$$(d)\ \int_{-\infty}^{+\infty} x^n \psi(x) dx = 0, \quad for\ 0 \le n < N; \tag{4}$$

$$(e)\ \sum_{l\in\mathbb{Z}} p_k \varphi(x-l) = 1; \tag{5}$$

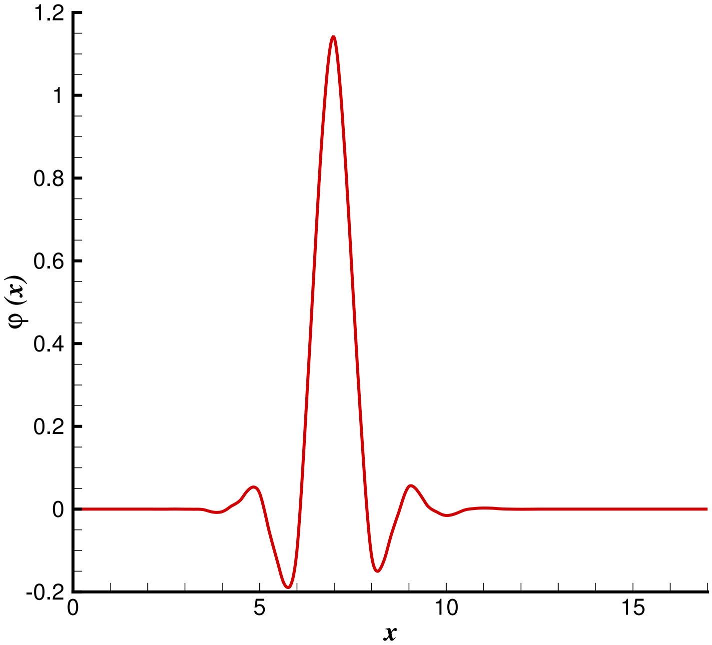


**Fig. 1.** Scaling function of the generalized Coiflet-type orthogonal wavelet with number of vanishing moment $N = 6$ and first order moment $M_1 = 7$.

where $p_k$ are the low-pass filter coefficients that can be found in [41,43], $N$ is the number of vanishing moment, and $M_n = \int_{-\infty}^{+\infty} x^n \varphi(x) dx$ is the nth-order moment of the scaling function. In this paper, the generalized Coiflet-type orthogonal wavelet with $N = 6, M_1 = 7$ is adopted. Note that the scaling function of the generalized Coiflet-type orthogonal wavelet has no analytical expression so that the values of this function are obtained using the procedure described in [30]. The basic graph of the scaling function $\varphi(x)$ is shown in Fig. 1. Using the above-mentioned scaling function, a multiresolution analysis [30,35] of the $L^2(\mathbb{R})$ can be constructed, which consists a sequence of nested subspaces $\{0\} \subset \cdots \subset \mathbb{V}_0 \subset \mathbb{V}_1 \subset \cdots \subset \mathbb{V}_j \subset \mathbb{V}_{j+1} \subset \cdots \subset L^2(\mathbb{R})$, where

$$\mathbb{V}_j = span\left\{\varphi(2^j x - l)\right\}_{l \in \mathbb{Z}}, \tag{6}$$

in which all the base functions are mutually orthogonal. Note that $j$ denotes the resolution level in the whole paper. Using the generalized Gaussian integral method developed by Zhou et al. [45], an arbitrary function $f(x) \in L^2(\mathbb{R})$ can be approximated by

$$f(x) \approx P^j f(x) = \sum_{l \in \mathbb{Z}} f\left(\frac{M_1 + l}{2^j}\right) \varphi(2^j x - l), \tag{7}$$

where $j$ denotes the resolution level.

Furthermore, through the boundary extension technique [30,34,42], the modified wavelet basis is constructed as

$$\varphi_{j,l}(x) = \begin{cases} \displaystyle\sum_{i=2-3N+M_1}^{-1} T_{0,l}\left(\frac{i}{2^j}\right)\varphi(2^j x - i + 7) + \varphi(2^j x - l + 7), & \\ \qquad\qquad\qquad\qquad\qquad\qquad l \in [0, 3], & \\ \varphi(2^j x - l + 7), \qquad\qquad\qquad l \in [4, 2^j - 4], & \\ \displaystyle\sum_{i=2^j+1}^{2^j-1+M_1} T_{1,2^j-l}\left(\frac{i}{2^j}\right)\varphi(2^j x - i + 7) + \varphi(2^j x - l + 7), & \\ \qquad\qquad\qquad\qquad\qquad\qquad l \in [2^j - 3, 2^j], & \end{cases} \tag{8}$$

where

$$T_{0,l}(x) = \sum_{i=0}^{3} \frac{p_{0,i,l}}{i!} x^i \ , \ T_{1,l}(x) = \sum_{i=0}^{3} \frac{p_{1,i,l}}{i!} (x - 1)^i, \tag{9}$$

and coefficients $p_{0,\,i,\,l}$ and $p_{1,\,i,\,l}$ are assigned as

$$\mathbf{P_0} = \begin{bmatrix} 1 & 0 & 0 & 0 \\ -11/6 & 3 & -3/2 & 1/3 \\ 2 & -5 & 4 & -1 \\ -1 & 3 & -3 & 1 \end{bmatrix}, \tag{10}$$

$$\mathbf{P_1} = \begin{bmatrix} 1 & 0 & 0 & 0 \\ 11/6 & -3 & 3/2 & -1/3 \\ 2 & -5 & 4 & -1 \\ 1 & -3 & 3 & -1 \end{bmatrix} \tag{11}$$

through relations $\mathbf{P_0} = \{2^{-ij} p_{0,i,l}\}$ and $\mathbf{P_1} = \{2^{-ij} p_{1,i,l}\}$ with $i = 0, 1, 2, 3$.

Using the modified wavelet base functions (8) and considering that the scaling function $\varphi(x)$ has a support interval [0, 17], an arbitrary bounded function $f(x) \in L^2[0, 1]$ can be approximated as

$$f(x) \approx P^j f(x) = \sum_{l=0}^{2^j} f\left(\frac{l}{2^j}\right) \varphi_{j,l}(x), \tag{12}$$

where $P^j$ is a projection operator on the subspace $\mathbb{V}_j$. Then, the derivative of the function can be approximated by

$$f^{(n)}(x) \approx \frac{d^n[P^j f(x)]}{dx^n} = \sum_{l=0}^{2^j} f\left(\frac{l}{2^j}\right) \varphi_{j,l}^{(n)}(x), \tag{13}$$

where the values of $\varphi_{j,l}^{(n)}(x)$ on equinoxes can be calculated through the method described in [30]. These two properties provide us a rather convenient way to express a known function by means of the wavelet.

According to [41,46], the accuracy of the approximation (12) and its derivatives (13) can be estimated by the following lemma:

**Lemma 1.** *For $f(x) \in L^2([0, 1]) \bigcap C^N([0, 1])$, the accuracy of the approximation (12) and its derivative (13) can be estimated as*

$$\left\| \frac{d^n f(x)}{dx^n} - \frac{d^n P^j f(x)}{dx^n} \right\|_{L^2} \le C\, 2^{-j(N-n)}, \tag{14}$$

*where $C$ is a positive constant that depends only on the function $f(x)$ and low-pass filter coefficients $p_k$, $N$ is the number of vanishing moment, and $0 \le n < N$.*

## 3. Basic ideas of the wHAM

To illustrate the basic ideas of the wHAM, let us consider the one-dimensional Bratu equation

$$\frac{d^2 u(x)}{dx^2} + \lambda e^{u(x)} = 0, \qquad x \in (0, 1), \tag{15}$$

with the boundary conditions

$$u(0) = u(1) = 0, \tag{16}$$

where $\lambda$ is a positive number, known as the Frank–Kamenetskii parameter [47]. Bratu's equation is used in a large variety of applications such as the fuel ignition model of the thermal combustion theory, the model of thermal reaction process, the Chandrasekhar model of the expansion of the Universe, questions in geometry and relativity about the Chandrasekhar model, chemical reaction theory, radiative heat transfer, nanotechnology, and so on [47].

In accordance with [47–49], there exist two known bifurcated solutions for $0 < \lambda < \lambda_c$, no solutions for $\lambda > \lambda_c$ and a unique solution when $\lambda = \lambda_c$, where $\lambda_c \approx 3.513830719$. For simplicity, the lower branch of the solution when $0 < \lambda < \lambda_c$ is considered in this paper. In the case of $0 < \lambda < \lambda_c$, the Bratu's equation has analytical solution in the following form:

$$u(x) = -2ln\left[\frac{\cosh(\frac{\theta}{2}(x - \frac{1}{2}))}{\cosh(\frac{\theta}{4})}\right], \tag{17}$$

where the constant $\theta$ is determined by the algebraic equation

$$\theta = \sqrt{2\lambda} \cosh\left(\frac{\theta}{4}\right). \tag{18}$$

Note that Bratu's equation (15) contains a transcendental nonlinear term $e^{u(x)}$, which leads to the complexity for the calculation of right-hand side term in the frame of HAM, as mentioned in [3,5]. In order to simplify the calculation, let us first introduce the following transformation

$$V(x) = \exp\left[-\frac{1}{2}u(x)\right]. \tag{19}$$

Then, the Bratu's equation (15) can be rewritten as

$$V(x)\frac{d^2V(x)}{dx^2} - \left(\frac{dV(x)}{dx}\right)^2 - \frac{\lambda}{2} = 0, \qquad x \in (0,1), \tag{20}$$

with the boundary conditions

$$V(0) = V(1) = 1. \tag{21}$$

In this form, the right-hand side in the HAM can be calculated much more efficiently. The solution of the original equation (15) can be obtained by the inverse transformation

$$u(x) = -2lnV(x). \tag{22}$$

### 3.1. Basic HAM

The HAM is essentially based on the homotopy, a basic concept of topology, which describes a continuous deformation or variation from a topological space to another. Therefore, the foremost to use the HAM for the considered problem is to construct a continuous variation between two functions, i.e. the known initial guess $V_0(x)$ and the unknown solution $V(x)$. Let $q \in [0, 1]$ denote an embedding parameter for homotopy, $c_0$ the convergence-control parameter, $\mathscr{L}$ an auxiliary linear operator and $\mathscr{N}$ a nonlinear operator, respectively. Then a continuous variation (with respect to the embedding parameter $q \in [0, 1]$) from the initial guess $V_0(x)$ to the solution $V(x)$ can be built by means of the so-called zeroth-order deformation equation

$$(1-q)\mathscr{L}[\phi(x;q) - V_0(x)] = c_0 q \mathscr{N}[\phi(x;q)], \quad q \in [0,1], \tag{23}$$

subject to the boundary conditions

$$\phi(0;q) = \phi(1;q) = 1, \tag{24}$$

where

$$\mathscr{N}[\phi(x;q)] = \phi(x;q)\frac{\partial^2\phi(x;q)}{\partial x^2} - \left(\frac{\partial\phi(x;q)}{\partial x}\right)^2 - \frac{\lambda}{2}. \tag{25}$$

Obviously, we have the solution $\phi(x;0) = V_0(x)$ when $q = 0$, and $\phi(x;1) = V(x)$ when $q = 1$, respectively. In other words, $\phi(x; q)$ denotes a continuous variation from the initial guess $V_0(x)$ to the solution $V(x)$, as $q$ increases from 0 to 1. Then, expand $\phi(x; q)$ in Maclaurin series with respect to the embedding parameter $q$, i.e.

$$\phi(x;q) = V_0(x) + \sum_{k=1}^{+\infty} V_k(x) q^k, \tag{26}$$

where

$$V_k(x) = \mathscr{D}_k[\phi(x;q)] = \frac{1}{k!}\frac{\partial^k\phi(x;q)}{\partial q^k}\bigg|_{q=0}. \tag{27}$$

Here, $\mathscr{D}_k[\phi]$ is called the mth-order homotopy-derivative operator of $\phi$, as defined by Liao [5]. Assuming that the auxiliary linear operator $\mathscr{L}$ and especially the convergence-control parameter $c_0$ is so properly chosen that the Maclaurin series (26) converges at $q = 1$, we gain the series solution

$$V(x) = V_0(x) + \sum_{k=1}^{+\infty} V_k(x). \tag{28}$$

And the corresponding $m$th-order approximation is given by

$$V(x) \approx \tilde{V}_m(x) = V_0(x) + \sum_{k=1}^{m} V_k(x). \tag{29}$$

Taking the $m$th-order homotopy-derivative operator on both sides of the zeroth-order deformation equation (24) as well as the boundary conditions (31), we have the $m$th-order deformation equation

$$\mathscr{L}[V_m(x) - \chi_m V_{m-1}(x)] = c_0\, R_m(x), \tag{30}$$

subject to the boundary conditions

$$V_m(0) = V_m(1) = 0, \tag{31}$$

where

$$\begin{aligned} R_m(x) &= \mathscr{D}_{m-1}\{\mathscr{N}[\phi(x;q)]\} \\ &= \sum_{k=0}^{m-1}\left[V_k(x)V''_{m-1-k}(x) - V'_k(x)V'_{m-1-k}(x)\right] - \frac{\lambda}{2}(1-\chi_m) \end{aligned} \tag{32}$$

and

$$\chi_k = \begin{cases} 0, & k \le 1, \\ 1, & k > 1. \end{cases} \tag{33}$$

Therefore, by the HAM, the original nonlinear problem described by Eqs. (20) and (21) is transformed into an infinite number of linear sub-problems governed by Eqs. (30) and (31). Note that, unlike perturbation techniques, such kind of transformation has nothing to do with any small/large physical parameters.

Besides, unlike perturbation techniques, the HAM provides us great freedom to choose the initial guess, the auxiliary linear operator and so on. According to the boundary conditions (21), the initial guess $V_0(x)$ can be chosen in the simplest form

$$V_0(x) = 1. \tag{34}$$

Since the highest-order derivative of Eq. (20) is second-order, we choose the auxiliary linear operator

$$\mathscr{L}[\phi(x;q)] = \frac{\partial^2\phi(x;q)}{\partial x^2} + \kappa_1\frac{\partial\phi(x;q)}{\partial x} + \kappa_0\phi(x;q), \tag{35}$$

where $\kappa_0$ and $\kappa_1$ are two constants to be chosen later.

### 3.2. High-order wavelet-Galerkin equation

The solution $V(x)$ can be expressed by many different base functions, such as polynomial series, trigonometric series, Chebyshev polynomial series and so on. The key point of the wHAM is to use the modified wavelet base functions (8) to express the solution.

Using the properties (12) and (13) of the modified wavelet base functions (8) and considering the boundary conditions (31), the function $V_m(x)$ and the right-hand side term in the $m$th-order ($m \ge 1$) deformation equation (30) can be approximated by

$$V_m(x) \approx P^j V_m(x) = \sum_{l=0}^{2^j} V_m\left(\frac{l}{2^j}\right)\varphi_{j,l}(x) = \sum_{l=1}^{2^j-1} V_m\left(\frac{l}{2^j}\right)\varphi_{j,l}(x), \tag{36}$$

and

$$R_m(x) \approx P^j R_m(x) = \sum_{l=0}^{2^j} R_m\left(\frac{l}{2^j}\right)\varphi_{j,l}(x), \tag{37}$$

where

$$R_m\left(\frac{l}{2^j}\right) = \sum_{k=0}^{m-1}\left[V_k\left(\frac{l}{2^j}\right)V''_{m-1-k}\left(\frac{l}{2^j}\right) - V'_k\left(\frac{l}{2^j}\right)V'_{m-1-k}\left(\frac{l}{2^j}\right)\right] - \frac{\lambda}{2}(1-\chi_m), \tag{38}$$

in which the derivatives can be approximated by

$$V_m^{(n)}(x) \approx \frac{d^n P^j V_m(x)}{dx^n} = \sum_{l=1}^{2^j-1} V_m\left(\frac{l}{2^j}\right)\varphi_{j,l}^{(n)}(x), \quad m \ge 1,\ n = 1, 2. \tag{39}$$

In addition,

$$V_0^{(n)}(0) = 0, \quad n = 1, 2. \tag{40}$$

Note that the boundary condition (31) is embedded in (36). In other words, the expressions (36) satisfies the boundary condition (31).

Substituting (36) and (37) into (30), we have the $m$th-order deformation equation in the wavelet form:

$$\sum_{l=1}^{2^j-1}\left[V_m\left(\frac{l}{2^j}\right)-\chi_m V_{m-1}\left(\frac{l}{2^j}\right)\right]\mathscr{L}\left[\varphi_{j,l}(x)\right]$$
$$=c_0\sum_{l=0}^{2^j}R_m\left(\frac{l}{2^j}\right)\varphi_{j,l}(x). \tag{41}$$

Since the wavelet approximation (36) of $V_m(x)$ satisfies the boundary conditions (31), (41) needs no additional boundary condition at all.

To solve the $m$th-order deformation equation (41) in the wavelet form, the Galerkin method is applied, where the base functions

$$\varphi_{j,k},\quad k=1,2,\cdots,2^j-1$$

are taken as weight functions. Multiplying both sides of Eq. (41) by $\varphi_{j,\,k}\ \left(k=1,2,\cdots,\ 2^j-1\right)$, respectively, and integrating over the interval [0,1], we have the $m$th-order wavelet-Galerlin deformation equation

$$\mathbf{A}\left(\hat{\mathbf{V}}_m-\chi_m\hat{\mathbf{V}}_{m-1}\right)=c_0\,\mathbf{B}\,\hat{\mathbf{R}}_m, \tag{42}$$

where

$$\hat{\mathbf{V}}_k=\left\{V_k\left(\frac{1}{2^j}\right),V_k\left(\frac{2}{2^j}\right),\cdots,V_k\left(\frac{2^j-1}{2^j}\right)\right\}^T \tag{43}$$

is a $(2^j-1)$-dimensional vectors,

$$\hat{\mathbf{R}}_m=\left\{R_m\left(\frac{0}{2^j}\right),R_m\left(\frac{1}{2^j}\right),R_m\left(\frac{2}{2^j}\right),\cdots,R_m\left(\frac{2^j-1}{2^j}\right),R_m(1)\right\}^T \tag{44}$$

is a $(2^j+1)$-dimensional vector,

$$\mathbf{A}=\left\{a_{k,l}=\int_0^1\mathscr{L}\left[\varphi_{j,l}(x)\right]\varphi_{j,k}(x)dx\right\}_{k,l=1}^{k,l=2^j-1} \tag{45}$$

and

$$\mathbf{B}=\left\{b_{k,l}=\int_0^1\varphi_{j,l}(x)\varphi_{j,k}(x)dx\right\}_{k=1,\quad l=0}^{k=2^j-1,\quad l=2^j+1} \tag{46}$$

are $(2^j-1)\times(2^j-1)$ and $(2^j-1)\times(2^j+1)$ constant matrices, respectively. Define the so-called generalized connection coefficients [41]:

$$\Gamma_{l,k}^{j,n}=\int_0^1\frac{d^n\varphi_{j,l}(x)}{dx^n}\varphi_{j,k}(x)dx. \tag{47}$$

Then, according to the definition (35) of the auxiliary linear operator, the matrix coefficients $a_{k,\,l}$ and $b_{k,\,l}$ can be rewritten as

$$\begin{cases}a_{k,l}=\Gamma_{l,k}^{j,2}+\kappa_1\Gamma_{l,k}^{j,1}+\kappa_0\Gamma_{l,k}^{j,0},\\ b_{k,l}=\Gamma_{l,k}^{j,0},\end{cases} \tag{48}$$

where the generalized connection coefficients can be obtained through the method described in [30]. For more details, please refer to [41]. Note that the matrices **A** and **B** are the same for all $m\geq 1$. So, it is computationally efficient to solve the $m$th-order wavelet-Galerlin deformation equation (42).

Solving the $m$th-order wavelet-Galerlin deformation equations (42) for $m=1,\,2,\,3,\,\cdots$ step by step, and then using (29), we have the $m$th-order wavelet approximation of the solution.

## 4. Results and analysis

Based on the exact solutions (17), we define the averaged square error $ErrSQ_m$ and the relative error $ErrRE_m(x)$ as follows:

$$ErrSQ_m=\frac{1}{2^j+1}\sum_{k=0}^{2^j}\left[\tilde{u}_m\left(\frac{k}{2^j}\right)-u_e\left(\frac{k}{2^j}\right)\right]^2, \tag{49}$$

$$ErrRE_m(x)=\frac{|\tilde{u}_m(x)-u_e(x)|}{|u_e(x)|},\quad 0<x<1, \tag{50}$$

where $\tilde{u}_m(x)$ is the $m$th-order wavelet approximation $\tilde{u}_m(x)=-2ln\tilde{V}_m$ in which $\tilde{V}_m$ is given by (29), and $u_e(x)$ is the lower branch of the exact solution, i.e. the solution in correspondence with the smaller value of $\theta$ in (18).

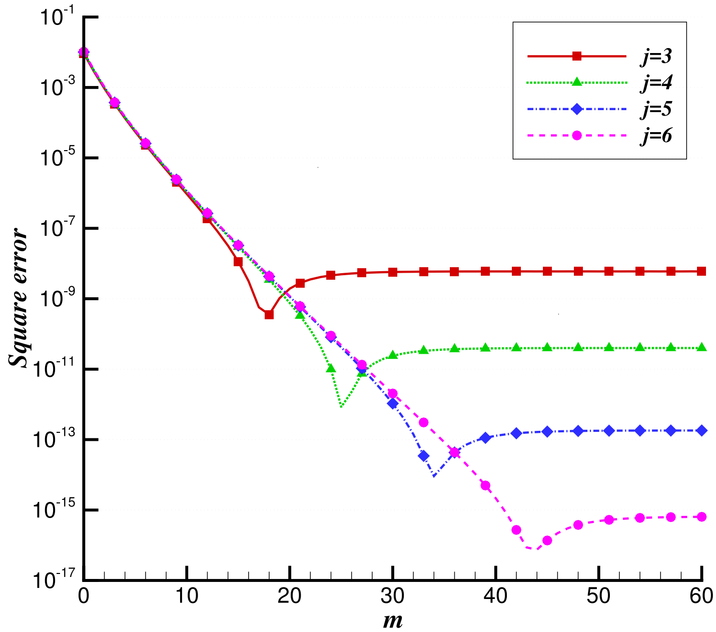


**Fig. 2.** The averaged square error of the wHAM wavelet approximations (given by different resolution level $j$) versus the approximation order $m$ by means of $c_0 = -1/2$ in case of the Frank–Kamenetskii parameter $\lambda = 1$, the auxiliary linear operator $\mathscr{L}[\phi(x;q)] = \frac{\partial^2\phi(x;q)}{\partial x^2}$ and the resolution level $j$ varying from 3 to 6. Solid line with square symbol: $j = 3$; dotted line with delta symbol: $j = 4$; dash-dotted line with diamond symbol: $j = 5$; dashed line and with circle symbol: $j = 6$.

### *4.1. Convergence of wavelet approximation*

Without loss of generality, let us first consider the cases of the Frank–Kamenetskii parameter $\lambda = 1$, the auxiliary linear operator $\mathscr{L}[\phi(x;q)] = \frac{\partial^2\phi(x;q)}{\partial x^2}$ and the resolution level $j$ varying from 3 to 6. In the frame of the wHAM, convergent series solution can be conveniently obtained by means of a proper value of the convergence-control parameter $c_0$. This is an advantage of the HAM, which differs the HAM from other analytic approximation techniques, as mentioned by Liao [2,3]. For comparison, $c_0 = -0.5$ is used here for the results reported below.

Fig. 2 shows the averaged square error $ErrSQ_m$ versus the approximation order $m$ for the different resolution level $j$. Note that, for each resolution level, the averaged square error decreases exponentially until to a constant $ErrSQ_m^*$ that is dependent upon the resolution level $j$: the larger the value of $j$, the smaller the final error $ErrSQ_m^*$. Thus, as long as the resolution level is large enough, such as $j = 6$, and the order of approximation is high enough, the wavelet approximation given by the wHAM is rather accurate. This indicates the validity of the wHAM for the nonlinear boundary value problem.

It is found that if the linear operator is chosen as $\mathscr{L}[\phi(x;q)] = \frac{\partial^2\phi(x;q)}{\partial x^2}$ and the convergence-control parameter $c_0$ is chose in the interval

$$\mathbf{R}_c = \{c_0 | -0.5 \le c_0 < 0\}, \tag{51}$$

convergent wavelet series solution can be obtained at the different resolution levels for the different physical parameters $\lambda$ $(0 < \lambda \le \lambda_c)$ of the Bratu equation (15), as shown in Fig. 3 for the comparison between the exact solution and the 40th-order wHAM solutions with the resolution level $j = 4$.

### *4.2. Accuracy and efficiency control by means of the resolution level*

As mentioned in Section 2, for an arbitrary function $f(x) \in L^2([0,\ 1])$, its approximation with higher accuracy can be easily obtained by raising the resolution level $j$. Therefore, in the frame of the wHAM, the accuracy of the solution can be controlled by adjusting the resolution level $j$, as shown in Fig. 2. Of course, a higher resolution level needs more CPU time. To compare the CPU time, all of the results are gained using the same desktop, i.e. DELL Inspiron 3847, Intel(R) Core(TM) i5-4460 CPU@ 3.20 GHz, 8GB memory (SAMSUNG DDR3 1600 MHz). The averaged square errors and the corresponding CPU times (pre-calculation included) for the 60th-order wavelet approximation in correspondence with the resolution levels are shown in Table 1.

According to Table 1, a higher resolution level leads to more accurate approximations but more CPU time. Note that, as the resolution level $j$ enlarges, the solution accuracy increases exponentially but with the linearly increasing CPU times. It should be emphasized that less than one second of CPU time is needed for all cases. Therefore, the wHAM possesses rather

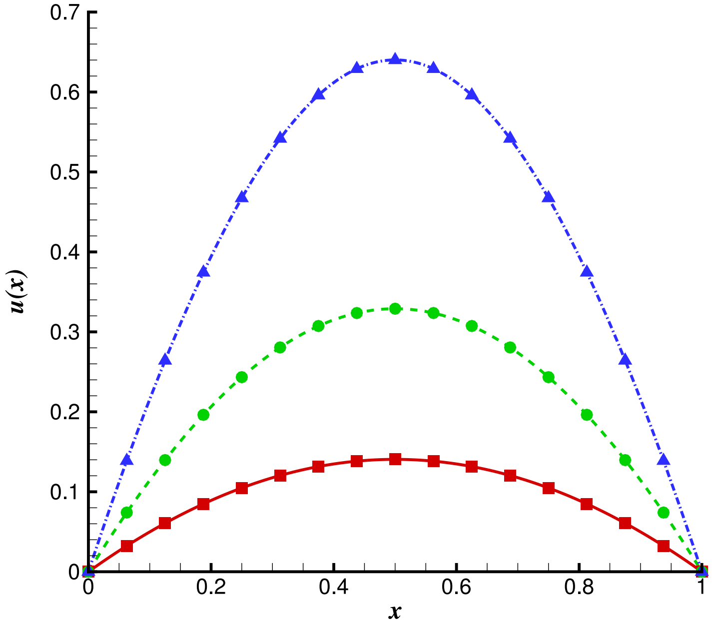


**Fig. 3.** Comparison between the 40th-order wHAM approximations and the exact solutions in case of $c_0 = -1/2$, the resolution level $j = 4$ and the auxiliary linear operator $\mathscr{L}[\phi(x;q)] = \frac{\partial^2\phi(x;q)}{\partial x^2}$. Solid line: exact solution when $\lambda = 1$; dashed line: exact solution when $\lambda = 2$; dash-dotted line: exact solution when $\lambda = 3$; square: wHAM approximation when $\lambda = 1$; circle: wHAM approximation when $\lambda = 2$; delta: wHAM approximation when $\lambda = 3$.

**Table 1**
The averaged square error and the CPU time (pre-calculation included) for the 60th-order wavelet approximation versus the resolution level $j$ in case of $\lambda = 1$, the convergence-control parameter $c_0 = -1/2$ and the auxiliary linear operator $\mathscr{L}[\phi(x;q)] = \frac{\partial^2\phi(x;q)}{\partial x^2}$.

| The resolution level $j$ | $ErrSQ_{60}$ | CPU time (sec.) |
|---|---|---|
| 2 | $2.839993 \times 10^{-08}$ | 0.152649 |
| 3 | $5.975293 \times 10^{-09}$ | 0.295230 |
| 4 | $3.986239 \times 10^{-11}$ | 0.368240 |
| 5 | $1.814512 \times 10^{-13}$ | 0.517127 |
| 6 | $6.509588 \times 10^{-16}$ | 0.920077 |

**Table 2**
Comparison of the averaged square error and the CPU time (pre-calculation included) at the different order of approximation $m$ given by the wHAM and the normal HAM in case of $\lambda = 1$, the convergence-control parameter $c_0 = -1/2$ and the auxiliary linear operator $\mathscr{L}[\phi(x;q)] = \frac{\partial^2\phi(x;q)}{\partial x^2}$.

| $m$ | $ErrSQ_m$ | | CPU time (second) | |
|---|---|---|---|---|
| | wHAM | HAM | wHAM | HAM |
| 5 | $6.083516 \times 10^{-05}$ | $1.196418 \times 10^{-04}$ | 0.902078 | 0.035024 |
| 10 | $1.155250 \times 10^{-06}$ | $5.574128 \times 10^{-06}$ | 0.904739 | 0.080574 |
| 20 | $1.180741 \times 10^{-09}$ | $2.806097 \times 10^{-08}$ | 0.908879 | 0.266205 |
| 30 | $2.039350 \times 10^{-12}$ | $2.337982 \times 10^{-10}$ | 0.911481 | 0.698994 |
| 40 | $2.159067 \times 10^{-15}$ | $2.492056 \times 10^{-12}$ | 0.914309 | 1.614642 |
| 50 | $4.885205 \times 10^{-16}$ | $3.072730 \times 10^{-14}$ | 0.917086 | 3.578035 |

high computational efficiency. In practical applications, it is necessary to balance the accuracy and computational efficiency. Fortunately, in the frame of the wHAM, the resolution level provides us a convenient way to obtain accurate enough approximations with satisfactory accuracy in a reasonable computational times. Therefore, in the frame of the wHAM, the accuracy and the computational efficiency can be conveniently controlled by means of adjusting the resolution level.

To further show the advantages of the wHAM, a comparison between the wHAM and the normal HAM is made, as shown in Table 2. Obviously, the wHAM approximation converges faster than that given by the normal HAM. Besides, the CPU times increases exponentially for the normal HAM. However, for the wHAM, most of the CPU time (about 0.9 s) is

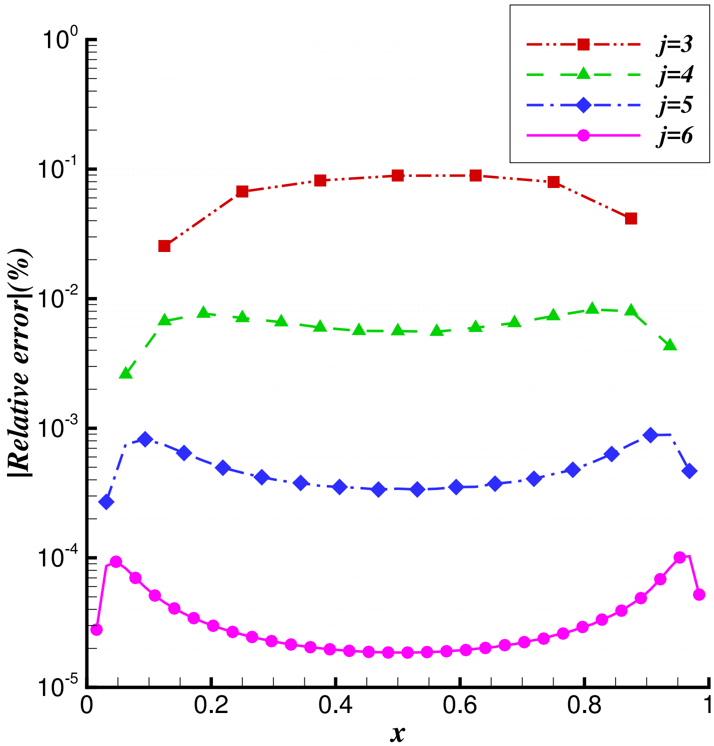


**Fig. 4.** The relative error distributions given by means of the wHAM in the different resolution level $j$ in case of $\lambda = 1$, $c_0 = -1/2$ and the auxiliary linear operator $\mathscr{L}[\phi(x;q)] = \frac{\partial^2\phi(x;q)}{\partial x^2}$. Dash-dot-dotted line: $j = 3$; dashed line: $j = 4$; dash-dotted line: $j = 5$; solid line: $j = 6$.

actually consumed for the pre-calculation of the connection coefficient matrixes, and it takes only 0.015 s more CPU time to gain the 50th-order approximation than the 10th-order ones! Thus, the wHAM is computationally rather efficient.

Another important problem for the wavelet approximation is the boundary leaping phenomenon [30,40,41], say, the error of approximation solution increases sharply near the boundary of the interval. However, for a good approximation, the relative error is expected to be evenly distributed. For this purpose, the boundary extension technique [30] is used, so that this boundary leaping phenomenon can be overcome, as shown in Fig. 4. This further verifies the validity of the wHAM and illustrates the convenience of controlling the accuracy by means of the resolution level in the frame of the wHAM.

In summary, since the wavelet is based on the multi-resolution analysis, the resolution level $j$ provides us a convenient way to balance the approximation accuracy and the computational efficiency. And thanks to the high approximation accuracy of the generalized Coiflet-type orthogonal wavelet, the wHAM is computationally rather efficient. The comparison between the wHAM and the normal HAM shows that the wHAM has indeed some obvious advantages in both of convergence rate and computational efficiency.

### *4.3. Non-sensitivity on the choice of the auxiliary linear operator*

Generally speaking [2,3], the HAM possesses the advantage of the flexibility on the choice of the auxiliary linear operator. In the frame of the normal HAM, however, the choice of the auxiliary linear operator is strongly dependent upon base functions of solution. In this paper, the second-order linear operator (35) containing two parameters $\kappa_0$ and $\kappa_1$ is used for the considered problem. When $\kappa_1 = \kappa_0 = 0$, power functions should be chosen as base functions; when $\kappa_1 = 0$ and $\kappa_0 > 0$, trigonometric functions should be used; when $\kappa_1 = 0$ and $\kappa_0 < 0$, exponential functions should be chosen, respectively. However, when $\kappa_1 \neq 0$, it becomes extremely difficult to choose a proper base function.

Fortunately, in the frame of the wHAM, the wavelet is always the base function, no matter what kind of the auxiliary linear operator is used. Without loss of generality, let us consider here three different types of auxiliary linear operators: $\mathscr{L}[\phi(x;q)] = \frac{\partial^2\phi(x;q)}{\partial x^2}$, $\mathscr{L}[\phi(x;q)] = \frac{\partial^2\phi(x;q)}{\partial x^2} + 5\phi(x;q)$ and $\mathscr{L}[\phi(x;q)] = \frac{\partial^2\phi(x;q)}{\partial x^2} + 5\frac{\partial\phi(x;q)}{\partial x} + 5\phi(x;q)$. Generally speaking, it is more time-consuming in the frame of the normal HAM to gain a trigonometric series or exponential series approximation than a power series approximation. However, in the frame of the wHAM, the CPU time is almost the same by means of the different types of the auxiliary linear operators, as shown in Fig. 5. More importantly, the CPU time increases linearly with respect to the order of approximation. In contrast, as shown in Fig. 6, the CPU time increases exponentially by the normal HAM, which may cause serious time-consumption. Note that, to obtain the 100th-order approximation, the wHAM needs only one second CPU times, while the normal HAM may cost 70 s! In practice, it is always necessary to calculate high order

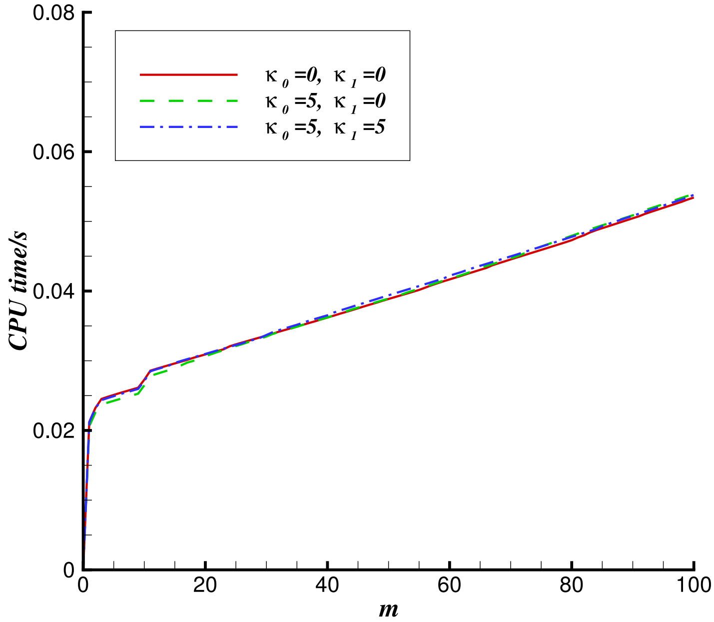


**Fig. 5.** The CPU time (pre-calculation not included) versus the approximation order $m$ by means of the wHAM in case of $\lambda = 1$, the resolution level $j = 6$ and the different types of auxiliary linear operators. Solid line: $\kappa_0 = 0, \kappa_1 = 0$; dashed line: $\kappa_0 = 5, \kappa_1 = 0$; dash-dotted line: $\kappa_0 = 5, \kappa_1 = 5$.

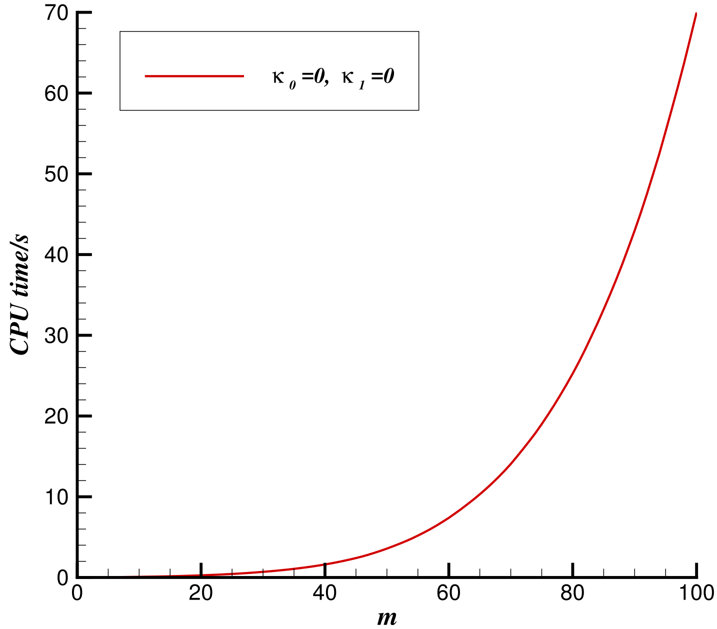


**Fig. 6.** The CPU time (no pre-calculation) versus approximation order $m$ by means of the normal HAM in case of $\lambda = 1$, the resolution level $j = 6$ and the auxiliary linear operator defined by $\kappa_0 = 0, \kappa_1 = 0$.

approximations for complicated nonlinear problems. Therefore, this property of the wHAM is of great significance. This is another advantage of the wHAM.

To illustrate the validity of the wHAM for the different auxiliary linear operators, let us further consider the case of $\kappa_1 = 0$ with $\kappa_0$ varying from $-5$ to 5. The averaged square errors versus the order of approximation $m$ are as shown in Fig. 7. Note that for each $\kappa_0$, the wavelet approximation given by the wHAM converges quickly to the exact solution. Thus, the validity of the wHAM seems to be not sensitive to the choice of the auxiliary linear operator. However, the convergence rate of the wHAM is indeed dependent upon the auxiliary linear operator: the larger the value of $\kappa_0$, the faster it converges, as shown in Fig. 7.

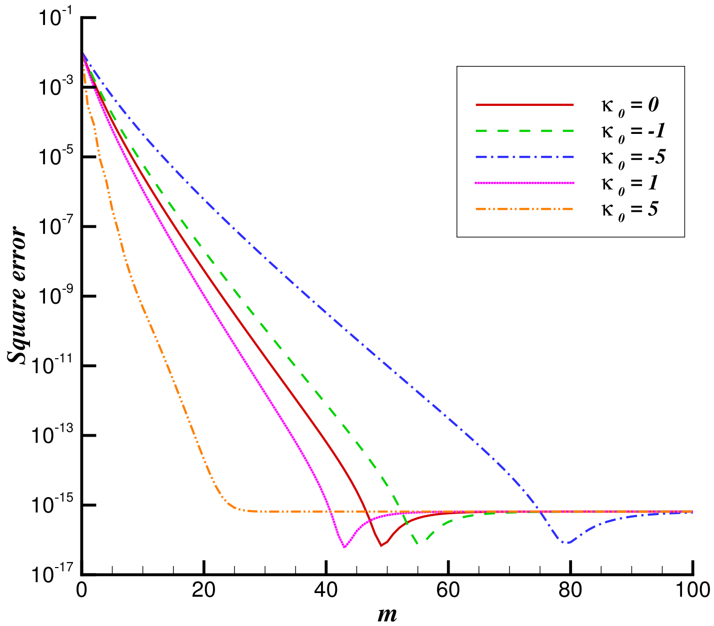


**Fig. 7.** The averaged square errors versus the order of approximation $m$ in case of $\lambda = 1$, the resolution level $j = 6$, $c_0 = -0.4$ and the different auxiliary linear operators ($\kappa_1 = 0$ with $\kappa_0$ varying from $-5$ to 5). Solid line: $\kappa_0 = 0$; dashed line: $\kappa_0 = -1$; dash-dotted line: $\kappa_0 = -5$; dotted line: $\kappa_0 = 1$; dash-dot-dotted line: $\kappa_0 = 5$.

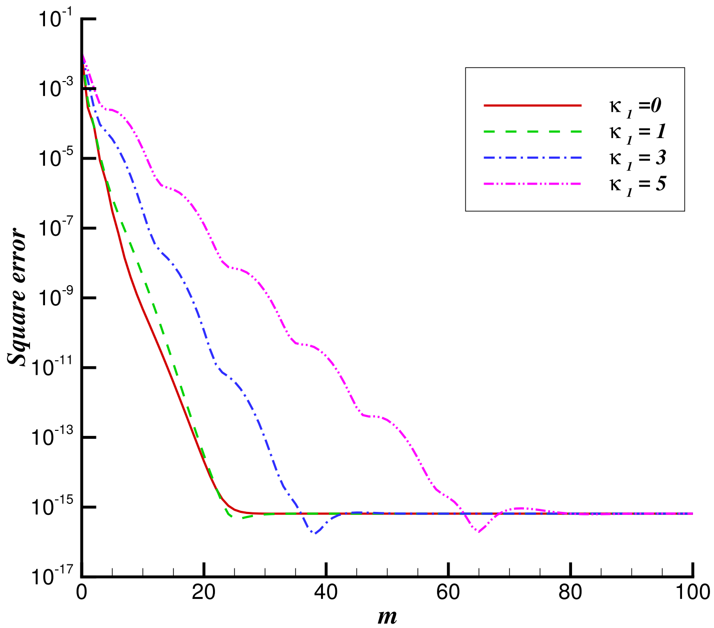


**Fig. 8.** The averaged square errors versus the order of approximation $m$ in case of $\lambda = 1$, the resolution level $j = 6$, $c_0 = -0.4$ and the different auxiliary linear operators ($\kappa_0 = 5$ with $\kappa_1$ varying from 0 to 5). Solid line: $\kappa_1 = 0$; dashed line: $\kappa_1 = 1$; dash-dotted line: $\kappa_1 = 3$; dash-dot-dotted line: $\kappa_1 = 5$.

Furthermore, let us consider the auxiliary linear operator in a more general form, i.e. $\mathscr{L}[\phi(x;q)] = \frac{\partial^2\phi(x;q)}{\partial x^2} + \kappa_1\frac{\partial\phi(x;q)}{\partial x} + \kappa_0\phi(x;q)$ in case of $\kappa_0 = 5$ with $\kappa_1$ varying from 0 to 5. The averaged square error versus the order of approximation $m$ when $\kappa_1 = 0, 1, 3, 5$ are as shown in Fig. 8. Note that in all considered cases we gain convergent results quickly, although the convergence rate is dependent upon the value of $\kappa_1$: the results given by $\kappa_1 = 0$ and $\kappa_1 = 1$ converge faster than others.

In fact, the normal HAM also provides us great freedom to choose the auxiliary linear operator. However, in the frame of the normal HAM, the base function is highly dependent upon the auxiliary linear operator. In the frame of the wHAM, the base function is always the wavelet function and the validity of the wHAM is not sensitive to the choice of the auxiliary

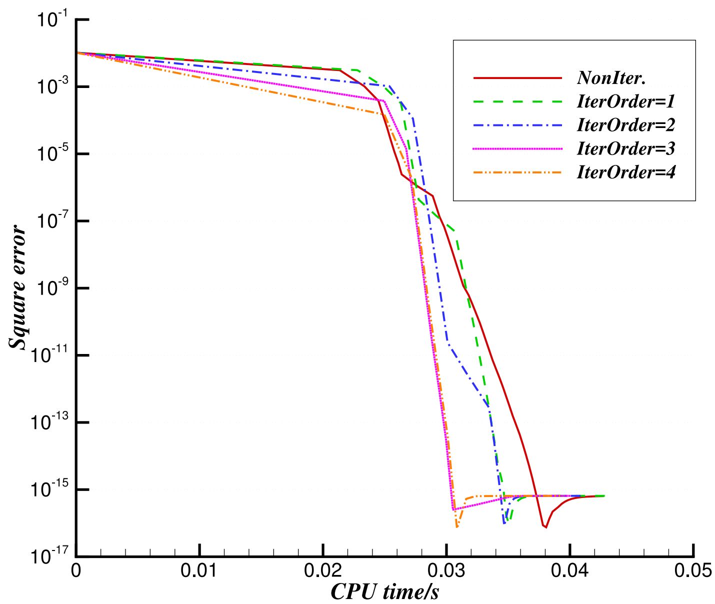


**Fig. 9.** Comparison of the square error curves of iterative and non-iterative wHAM in case of $\lambda = 1$, the resolution level $j = 6$ and $\kappa_0 = \kappa_1 = 0$. Solid line: non-iterative result; dashed line: $IterOrder = 1$; dash-dotted line: $IterOrder = 2$; dotted line: $IterOrder = 3$ dash-dot-dotted line: $IterOrder = 4$.

linear operator, so that we have larger freedom to choose the auxiliary linear operator. So, it is convenient to search for a better auxiliary linear operator in the frame of the wHAM. This is another advantage of the wHAM.

### *4.4. Convergence acceleration by iteration*

In the frame of the normal HAM, it has been verified [3,24] that the iteration can greatly accelerate the convergence. However, in the wHAM, the CPU time increases linearly rather than exponentially with respect to the order of approximation, as shown in Fig. 5. Is the iteration still effective in the wHAM? To answer this question, the simplest second-order operator $\mathscr{L}[\phi(x;q)] = \frac{\partial^2\phi(x;q)}{\partial x^2}$ is chosen as the auxiliary linear operator.

Fig. 9 shows the averaged square error versus the CPU time (pre-calculation not included), given by the iterative and non-iterative wHAM. It is found that the iteration technique can indeed accelerate the convergence, too. Note that the 3rd and 4th-order iteration formulas leads to faster convergence than the 1st and 2nd-order ones. Therefore, the iteration is suggested in the wHAM, if necessary.

## 5. Concluding remarks and discussions

In this paper, a HAM-based wavelet approach for nonlinear ordinary differential equations, namely the wavelet homotopy analysis method (wHAM), is proposed, which successfully combines the homotopy analysis method, the generalized Coiflet-type orthogonal wavelet and the Galerkin method together. The one-dimensional Bratu's equation is used as an example to describe the basic ideas of the wHAM and to illustrate its validity. By means of choosing a proper value of the so-called convergence-control parameter, the wavelet approximations given by the wHAM with various auxiliary linear operators converge quickly to the exact solution.

It is found that the wHAM not only keeps the advantages of the normal HAM, but also possesses some new merits. First of all, the convergence-control parameter, which plays a significant role in the normal HAM, still provides us a convenient way to guarantee the convergence of the wavelet approximation in the wHAM. Secondly, since the wavelet approximation is based on multi-resolution analysis, the resolution level provides us a convenient way to balance the computational efficiency and approximative accuracy so that an accurate enough approximation can be obtained efficiently. Note that the convergent solutions for all cases considered in this paper can be gained in less than one second CPU times by means of the wHAM. This indicates that the wHAM possesses the high computational efficiency. Besides, different from the normal HAM, the CPU time of the wHAM just increases linearly with respect to the approximation order. Furthermore, in the frame of the wHAM, the base function is always the wavelet function and besides the validity of the wHAM is not sensitive to the choice of the auxiliary linear operator, so that the wHAM provides us larger freedom than the normal HAM to choose the auxiliary linear operator. Therefore, it is possible to choose an optimal auxiliary linear operator in the frame of the wHAM, which might lead to rather fast convergence rate. In addition, it is found that the iteration can greatly accelerate the convergence so that the computational efficiency can be further improved.

However, any method has shortages and limitations, so does the wHAM. As the computation is carried out numerically rather than analytically, it is not convenient to set the convergence-control parameter as an unknown parameter and to optimize it by means of minimizing the square residual errors. Besides, due to the high frequency oscillation of the derivatives of the scaling function, the wHAM is not suggested if the governing equation contains a derivative with an order higher than four. In addition, in the frame of the wHAM, it is unavoidable to calculate the derivatives of the scaling function, so the approximation accuracy might more or less be affected. All of these limitations are expected to be improved in future, which however do not limit the use of the wHAM for nonlinear boundary value problems with high nonlinearity.

## Acknowledgment

This work is partially supported by the National Natural Science Foundation of China (Approval No. 11272209 and 11432009).

## References

[1] Liao SJ. The proposed homotopy analysis technique for the solution of nonlinear problems. Shanghai Jiao Tong University; 1992. Ph.d thesis.
[2] Liao SJ. Beyond perturbation: introduction to the homotopy analysis method. CRC press; 2003.
[3] Liao SJ. Homotopy analysis method in nonlinear differential equations. New York: Springer-Verlag; 2011.
[4] Liao SJ. On the homotopy analysis method for nonlinear problems. Appl Math Comput 2004;147(2):499–513.
[5] Liao SJ. Notes on the homotopy analysis method: some definitions and theorems. Commun Nonlinear Sci Numer Simul 2009;14(4):983–97.
[6] Liao SJ. An optimal homotopy-analysis approach for strongly nonlinear differential equations. Commun Nonlinear Sci Numer Simul 2010;15(8):2003–16.
[7] Liao SJ. On the method of directly defining inverse mapping for nonlinear differential equations. Nume Algorithm 2015. (published online with doi: 10.1007/s11075-015-0077-4.)
[8] Vajravelu K, Gorder RAV. Nonlinear flow phenomena and homotopy analysis: fluid flow and heat transfer. Heidelberg: Springer; 2012.
[9] Abbasbandy S. The application of homotopy analysis method to nonlinear equations arising in heat transfer. Phys Lett A 2006;360(1):109–13.
[10] Hayat T, Ellahi R, Ariel PD, Asghar S. Homotopy solution for the channel flow of a third grade fluid. Nonlinear Dyn 2006;45:55–64.
[11] Gorder RAV, Vajravelu K. Analytic and numerical solutions to the lane-emden equation. Phys Lett A 2008;372:6060–5.
[12] Ghotbi AR, Omidvar M, Barari A. Infiltration in unsaturated soils – an analytical approach. Comput Geotech 2011;38:777–82.
[13] Nassar CJ, Revelli JF, Bowman RJ. Application of the homotopy analysis method to the poissonoltzmann equation for semiconductor devices. Commun Nonlinear Sci Numer Simulat 2011;16:2501–12.
[14] Mastroberardino A. Homotopy analysis method applied to electrohydrodynamic flow. Commun Nonlinear Sci Numer Simulat 2011;16:2730–6.
[15] Aureli M. A framework for iterative analysis of non-classically damped dynamical systems. J Sound Vibr 2014;333:6688–705.
[16] Sardanyés J, Rodrigues C, Januário C, Martins N, Gil-Gómez G, Duarte J. Activation of effector immune cells promotes tumor stochastic extinction: a homotopy analysis approach. Appl Math Comput 2015;252:484–95.
[17] Zou K, Nagarajaiah S. An analytical method for analyzing symmetry-breaking bifurcation and period-doubling bifurcation. Commun Nonlinear Sci Numer Simulat 2015;22:780–92.
[18] Gorder RAV. Relation between lanemden solutions and radial solutions to the elliptic heavenly equation on a disk. New Astron 2015;37:42–7.
[19] Kevorkian J, Cole JD. Perturbation methods in applied mathematics, vol. 34. Springer Science & Business Media; 2013.
[20] Nayfeh AH. Perturbation methods. John Wiley & Sons; 2008.
[21] Lyapunov AM. The general problem of the stability of motion. Int J Control 1992;55(3):531–4.
[22] Karmishin AV, Zhukov AI, Kolosov VG, et al. Methods of dynamics calculation and testing for thin-walled structures. Mashinostroyenie, Moscow 1990.
[23] Adomian G. Solving frontier problems of physics: the decomposition method, vol. 60. Springer Science & Business Media; 2013.
[24] Zhao YL, Lin ZL, Liao SJ. An iterative analytical approach for nonlinear boundary value problems in a semi-infinite domain. Comput Phys Commun 2013;184:2136–44.
[25] Motsa S, Sibanda P, Shateyi S. A new spectral-homotopy analysis method for solving a nonlinear second order BVP. Commun Nonlinear Sci Numer Simul 2010a;15(9):2293–302.
[26] Motsa S, Sibanda P, Awad F, Shateyi S. A new spectral-homotopy analysis method for the MHD jeffery–hamel problem. Comput Fluids 2010b;39(7):1219–25.
[27] Sibanda P, Motsa S, Makukula Z. A spectral-homotopy analysis method for heat transfer flow of a third grade fluid between parallel plates. Int J Numer Methods Heat Fluid Flow 2012;22(1):4–23.
[28] Motsa S. Application of the new spectral homotopy analysis method (sham) in the non-linear heat conduction and convective fin problem with variable thermal conductivity. Int J Comput Methods 2012;9(03):1250039.
[29] Nik HS, Effati S, Motsa SS, Shirazian M. Spectral homotopy analysis method and its convergence for solving a class of nonlinear optimal control problems. Numer Algorithms 2014;65(1):171–94.
[30] Wang JZ. Generalized theory and arithmetic of orthogonal wavelets and applications to researches of mechanics including piezoelectric smart structures. Lanzhou University; 2001. Ph.d thesis.
[31] Wang JZ, Zhou YH, Gao HJ. Computation of the laplace inverse transform by application of the wavelet theory. Commun Numer Methods Eng 2003;19(12):959–75.
[32] Wang JZ, Wang XM, Zhou YH. A wavelet approach for active-passive vibration control of laminated plates. Acta Mech Sin 2012;28(2):520–31.
[33] Liu XJ, Wang JZ, Zhou YH. A wavelet method for solving nonlinear time-dependent partial differential equations. CMES 2013;94(3):225–38.
[34] Liu XJ, Zhou YH, Zhang L, Wang JZ. Wavelet solutions of burgers equation with high reynolds numbers. Sci China Technol Sci 2014;57(7):1285–92.
[35] Daubechies I, et al. Ten lectures on wavelets, vol. 61. SIAM; 1992.
[36] Cui JT, Cheng ZX. Introduction to wavelet analysis. Xi'an Jiao Tong University Press ,China; 1995.
[37] Kosloff D, Kessler D, Filho A, Tessmer E, Behle A, Strahilevitz R. Solution of the equations of dynamic elasticity by a chebychev spectral method. Geophysics 1990;55(6):734–48.
[38] Jaffard S. Wavelet methods for fast resolution of elliptic problems. SIAM J Numer Anal 1992;29(4):965–86.
[39] Alpert B, Beylkin G, Coifman R, Rokhlin V. Wavelet-like bases for the fast solution of second-kind integral equations. SIAM J Sci Comput 1993;14(1):159–84.
[40] Xu J-C, Shann W-C. Galerkin-wavelet methods for two-point boundary value problems. Numerische Mathematik 1992;63(1):123–44.
[41] Liu XJ. A wavelet method for uniformly solving nonlinear problems and its application to quantitative research on flexible structures with large deformation. Lanzhou University; 2014. Ph.d thesis.
[42] Zhou YH, Wang XM, Wang JZ, Liu XJ. A wavelet numerical method for solving nonlinear fractional vibration, diffusion and wave equations. Comput Model Eng Sci 2011;77(2):137.
[43] Zhang L, Liu XJ, Zhou YH, Wang JZ. Influence of vanishing moments on the accuracy of a modified wavelet galerkin method for nonlinear boundary value problems. In: 11th International Conference of Numerical Analysis and Applied Mathematics 2013, vol. 1558. AIP Publishing; 2013. p. 942–5.

[44] Chen MQ, Hwang C, Shih YP. The computation of wavelet-galerkin approximation on a bounded interval. Int J Numer Methods Eng 1996;39(17):2921–44.
[45] Zhou YH, Wang JZ. Generalized gaussian integral method for calculations of scaling function transform of wavelets and its applications. Acta Math Scientia(Chinese Edition) 1999;19(3):293–300.
[46] Sweldens W, Piessens R. Quadrature formulae and asymptotic error expansions for wavelet approximations of smooth functions. SIAM J Numer Anal 1994;31(4):1240–64.
[47] Jacobsen J, Schmitt K. The liouville-bratu-gelfand problem for radial operators. J Differ Equ 2002;184(1):283–98.
[48] Buckmire R. Application of a mickens finite-difference scheme to the cylindrical bratu-gelfand problem. Numer Methods Partial Differ Equ 2004;20(3):327–37.
[49] Jalilian R. Non-polynomial spline method for solving bratu's problem. Comput Phys Commun 2010;181(11):1868–72.